

A Study of Robotic Grinding Path Planning

M. DIDI CHAOUI^a, F. LEONARD^b and G. ABBA^c

a. Université de Lorraine, Arts et Métiers ParisTech, mohamed.didi-chaoui@univ-lorraine.fr

b. Université de Lorraine, Arts et Métiers ParisTech, francois.leonard@univ-lorraine.fr

c. Université de Lorraine, Arts et Métiers ParisTech, gabriel.abba@univ-lorraine.fr

Résumé:

Dans cet article, nous proposons un système de meulage robotique capable de produire une pièce finie qui respecte certaines spécifications géométriques du produit. Il est composé d'un actionneur avec 1 ddl fixé entre la meuleuse et le robot. L'actionneur 1 ddl associé à l'outil de meulage peut être monté sur des installations robotiques existantes, ce qui rend cette solution très flexible et facile à utiliser par les industriels. Le système de rectification composé du robot et de l'actionneur peut appliquer une force de contact constante entre la pièce et l'outil. Une méthode de planification de chemin est également présentée dans cet article. À l'aide des calculs analytiques, la trajectoire du robot est déterminée pour le surfacage et le meulage d'angle d'une pièce parallélépipédique avec une précision donnée de la forme de la surface.

Abstract :

In this paper a robotic grinding system which can produce a finished workpiece that respects some product geometric specifications is proposed. It is composed of a 1 DoF active compliance actuator fixed between the grinder and the robot. The 1 DoF actuator associated to the tool can be mounted at existing robotic installations which make this solution very flexible and easy to use by the industrials. The grinding system composed of the robot and the actuator is able to apply a constant contact force between the workpiece and the grinding tool. A path planning method is also presented in this article. Using analytical calculations, the robot path is determined for surface and corner grinding of a parallelepiped workpiece with a given precision of the surface shape.

Keywords: Path planning, Robotic grinding, Angle grinding, Surface roughness, workpiece shaping.

1 Introduction

In order to reduce the number of tedious operations affected to the operators, to improve their working conditions by reducing dangerous operations and to improve quality consistency of manufactured workpieces, many industrials chose to automatize different kinds of processes. Grinding process is one of those processes that represented a serious problem [1] and [2]. Royal Society for the Prevention of Accidents Surveillance Systems data showed that angle grinders were the most dangerous tools with an average of 5,400 injuries recorded yearly in Great Britain. According to this research, the most injured areas are face, head and upper extremity [3]. Removal of Excess material, surfacing and creating rounds in workpieces are dangerous and time consuming grinding operations affected to skilled operators to do manually. These operations become a bigger problem when the size of the ground workpieces is very large. In literature,

proposed automation solutions can be categorized in two groups. The first group concerns the automation using CNC special-purpose machines, the second group concerns the automation using robots. But the first solution is normally quite expensive. Industrial robots have been proven to be a more economical solution for automation. The robot can be programmed to carry out the grinding jobs and can achieve the required surface quality and machining consistency with active contact force control. The existing active force control methods can be broadly categorized as through-the-arm and active end effector force control.

Through-the-arm force control is a well-known technique where force sensory feedback is used to determine the tool-to-part contact, and the robot's position is adjusted accordingly. One can immediately notice the combination of position and force control. This combination is referred to as hybrid control (or hybrid position/force control). [4] presents a robot control system dedicated to grinding large Francis turbines. The control system is based on an active force feedback system using a three axes force sensor attached to the robot's end effector. This system offers high flexibility and robustness against workpiece positioning and the grinding tool wear. Using the identified models, [5] developed and tested an adaptive pole placement controller using computer simulations. The purpose of the controller is to regulate the normal grinding force, see [6]. On the basis of a detailed analysis of the grinding process, motions of the constrained dynamic system of a grinding robot is modelled in this paper. In the model, the constrained generalized forces are included and expressed as an obvious function of the state and input generalized forces. A controller is then built without involving any force feedback sensors. Simulations have been done for justification of the feasibility of the controller by taking an articulated planar two-link manipulator as an example [7].

On the other hand, an active or passive compliance end effector control involves the end effector tooling having the ability to control the applied force by measuring the force error. This is done independently from the robot's position controller and depend only on the force control. In other words, the force and position control are dissociated in active control. Active compliance actuators can be classified as programmable and non-programmable. The programmable type can accomplish trajectory grinding-force tracking, whereas the non-programmable active end effectors cannot. A passive compliance tool would also be suitable, which refers to a tool composed of a particular material that enables compliance. To calculate the grinding force, a simplified grinding model is used and a path planning program determined the efficient path of the robot that minimizes the grinding time and achieve the wanted shape of the workpiece (Radius of the corners, surface roughness, etc).

2 Grinding system

Prior to modelling, a grinding system is developed. This system is composed of a serial robot and an active grinding end effector Fig. 1(a). The used robot is a 6 axis serial robot ABB IRB 7600 with a maximum carrying charge of 500 Kg. The grinding end-effector is attached to the end of arm of the robot. The grinding end-effector is equipped with a 1 DoF pneumatic cylinder attached to the angle grinder. The actuator allows the movement of the grinding tool along the Z axis. A rigid grinding wheel is mounted on the electric angle grinder.

Different grinding tool holders can be used by opening the chuck of the tool holder and inserting a different grinding tool. A diagram is shown in Fig. 1 (b) to illustrate the dynamic interaction involved in this system. Pressurized air and electric current enter the pneumatic cylinders and the angle grinder respectively. The air pressure causes the piston to extend, moving in the XZ plan the grinding tool toward the workpiece in a direction that creates an angle $\alpha=5^\circ$ with grinded surface. The main objective of the pneumatic actuator is to obtain a constant contact force. The electric current is supplied to the grinding wheel and determines its power output. Finally, based on the tool/part position, a particular material removal rate (MRR) is obtained.

The relationship between the normal grinding force and the grinding parameters is presented later in this paper.

3 Grinding process

We chose in this work a rounded corner grinding and surfacing of a large parallelepiped workpiece as case study. Such operations are usually done manually by industrial partners and can take several days to finish for a complex workpiece. This makes the process automation much needed. As an example in our case, we simplify the problem to grinding a radius $R=4\text{mm}$ on the corners and grinding a thickness of $D=0.1\text{mm}$ from the superior surface of the part (Fig. 1 (c)). The round is located as well on the superior surface of the parallelepiped workpiece. The grinding wheel will be at a constant angle α compared to the ground surface as illustrated in Fig. 2.

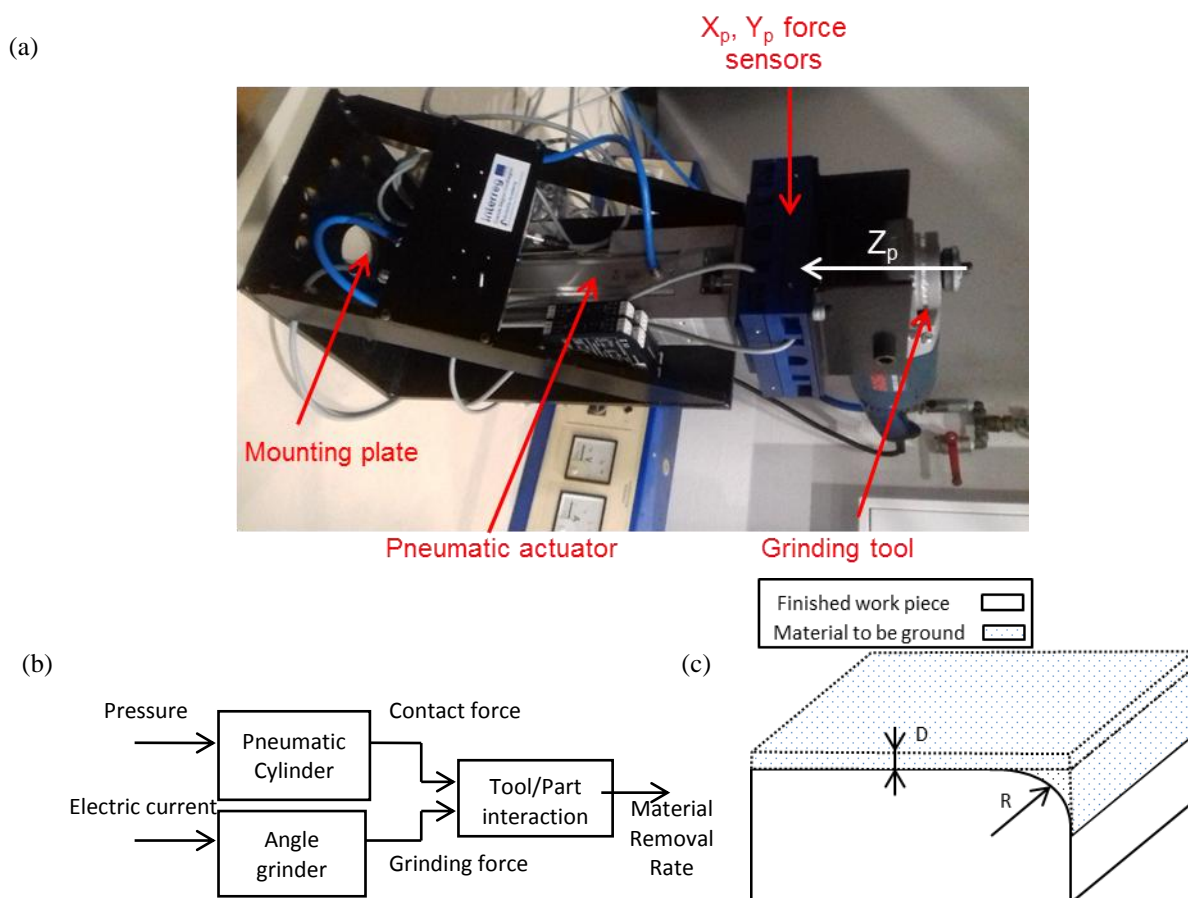


Fig. 1 (a) Active grinding end effector for robotic grinding

(b) Relation between the components of the grinding system (c) 4 mm rounded corner on the workpiece and 0.1 mm surfacing

The grinding process is done in two steps in order to reduce the needed time for this operation. The first step is roughing step, in which the material removal rate is maximized. The area of the contact surface between the grinding wheel and the workpiece is consequently maximized (S_{max}) taking into consideration different criterion. The second step is finishing operation. In this step the quality of the final surface is more important than the material removal rate.

4 Modeling of the grinding force

Grinding is a subject that gained great attention in the last decades. Many research works were interested in studying this process. Today, in the literature, numerous models are used to describe different parameters of the grinding operation. There are temperature models, force models, surface roughness models, energy models, etc.

The material removal rate, the dynamic behaviour of the grinding tools, the surface quality and tool wear are greatly influenced by the grinding forces, see [8]. Therefore, many research developments were focalized on calculating this latter.

[9] considered that grinding force model is directly linked to the shear strength of the grinded workpiece. [10] took into consideration the effect of the shape of the grinding wheel. [11] proposed a model that considered the distance between cutting edges of the grinding wheel. [12] used two different grinding models. The first model is used when the grinded material is easy to grind, the second one is used when the grinded material is hard to grind. [13] superimposed all instantaneous frictional and chip formation forces of the individual edges in contact with the workpiece. The grinding force model is derived as a function of the main grinding parameters. The model of the normal grinding force F_p has an exponent that is $\varepsilon=0.5$ when the phenomenon is purely frictional and it is $\varepsilon=1$ when the phenomenon is purely a chip formation force (1).

$$F_p = K_w [C_1]^\gamma \left[\frac{Q_w}{v_s} \right]^{2\varepsilon-1} [d]^{1-\varepsilon} [2R]^{1-\varepsilon} \quad (1)$$

Where, K_w is a proportionality factor, ε is an exponent taking values in the range of 0.5 to 1, γ is another exponent taking values from 0 to 1 depending on the grinding parameter and finally C_1 is the cutting edge density. Those experimental parameters must be determined according to the application. Q_w is the specific material removal rate, v_s is the grinding wheel speed, d is the cut depth and R is the radius of the grinding wheel.

Previous works supposed that grit distribution in the grinding wheel is uniform. [14] developed a stochastic grinding force model that considered the random distribution of grits.

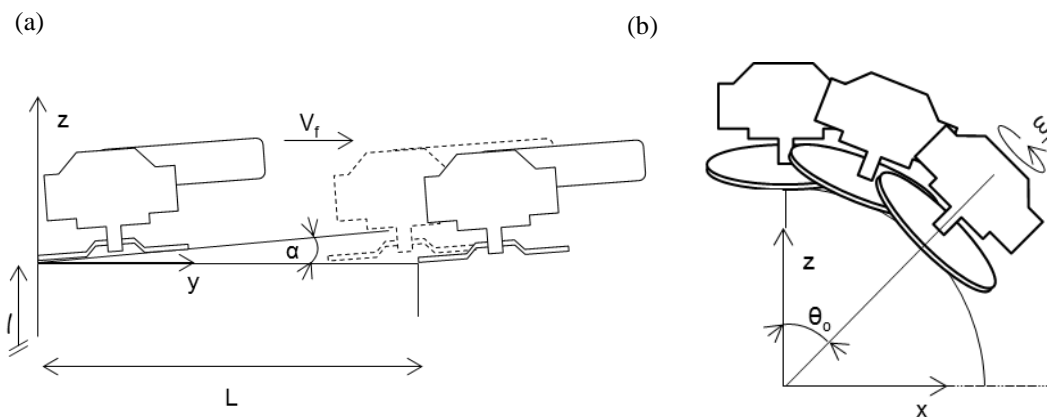


Fig. 2 (a) Grinding configuration in the YZ plan and (b) in the XZ plan

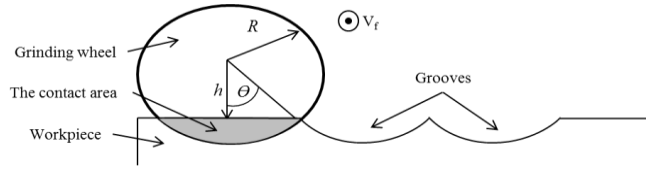


Fig. 3 Grinding tool in contact with the workpiece (the angle θ is exaggerated for illustration purposes)

The used process model for the chosen grinding application is that of [15] defined by eq. (2) with K_1 and K_2 experimentally determined. It is widely used for disc and cup grinding applications. This model is similar to the models proposed by [16] and [17]. For simulation and control, a simplification of the model is needed.

$$F_p' = K_1 + K_2 Q_w \quad (2)$$

In reality, the contact surface between the grinding wheel and the workpiece is small (Fig. 3), therefore the angle θ is very small and can be approximated using (3).

We have:

$$\sin\theta = \frac{\sqrt{R^2 - h^2}}{R} \approx \theta \quad (3)$$

$$R^2\theta \approx R\sqrt{R^2 - h^2} \quad (4)$$

And due to the tilt angle α of the grinding disc:

$$h = R - \frac{d}{\cos\alpha} \quad (5)$$

With d is the cut depth. The contact surface between the wheel and the workpiece is calculated by eq. (6)

$$S = 2R\sqrt{R^2 - h^2} \frac{\pi}{2\pi} - h\sqrt{R^2 - h^2} \quad (6)$$

Suppose that $R+h \approx 2R$ the equation can be transformed to:

$$S = (R - h)^{\frac{3}{2}} \sqrt{R + h} = (R - h)^{\frac{3}{2}} \sqrt{2R} = \left(R - \left(R - \frac{d}{\cos\alpha} \right) \right)^{\frac{3}{2}} \sqrt{2R} \quad (7)$$

The simplified force model can be then written as follows:

$$F_p' = K_1 + K_2 Q_w = K_1 + K_2 S V_f \quad (8)$$

$$F_p = K_2 S V_f = K_2 V_f \left(R - \left(R - \frac{d}{\cos\alpha} \right) \right)^{\frac{3}{2}} \sqrt{2R} = K d^{\frac{3}{2}} \quad (9)$$

Because α, R, V_f are constants.

With $K = \frac{K_2 V_s \sqrt{2R}}{(\cos\alpha)^{\frac{3}{2}}}$, $F_p = F_p' - K_1$ and $\beta = 3/2$.

The dynamic behaviour of the PA and the grinding process (9) were used to control the grinding system and are implemented in Matlab simulation in order to observe the dynamic behaviour of the system [18].

5 Path planning

5.1 Position of the grinding wheel

The grinding path can be described by defining the succession of point where the center of the grinding disc must be. The superior surface and the rounds while be ground in multiple layers that have the same thickness. Each layer is ground with multiple passes of the grinding wheel (Fig. 4). The number of layers and passes depends on the grinding process parameters as well as the grinding wheel and the workpiece geometry. The grinding wheel, while doing one pass will leave an elliptic groove on the surface of the workpiece (Fig. 3) due to the incline angle.

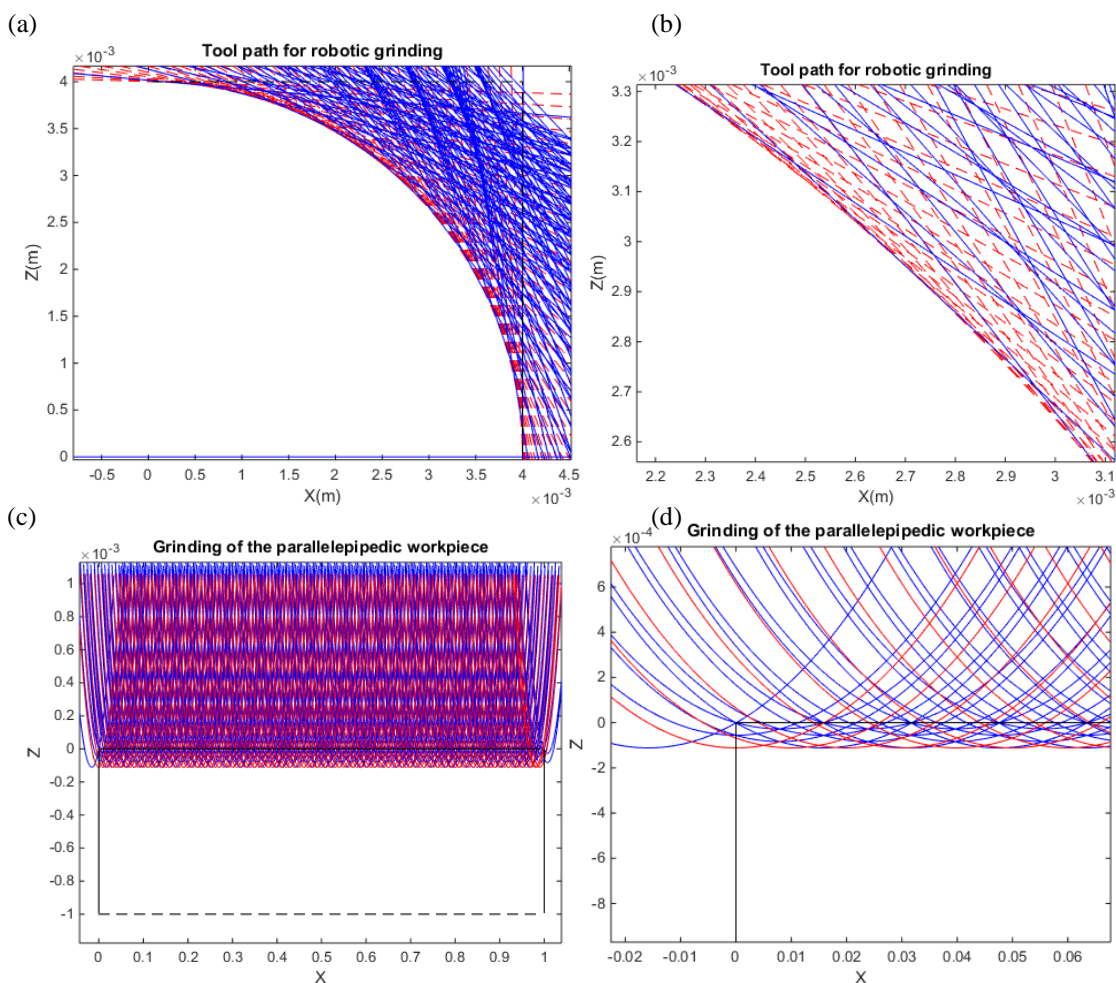


Fig. 4 (a) Edge of the grinding wheel in first step in blue and second step in red for corner grinding (b) close up look to the edges (c) Edge of the grinding wheel for surface grinding (d) close up look to the edges

In the first grinding step, the material removal rate must be maximized to reduce the time needed for this operation. Using the force model developed in the previous section(9), we can calculate the maximum cut depth d_{max} that the robot can do in order to have the maximum MRR for a given value of the grinding force F_p (in our case $F_p= 200N$). Using (7) we can calculate the surface area of the ellipse that is going to be emerged inside the workpiece (surface highlighted in grey colour in Fig. 3). This surface will help determine the position of the ellipse using (5). The next pass will be placed directly next to the first pass until the whole layer is covered. For the second layer and for the other layers, the grinding wheel will be placed between two passes of the previous layer as shown in Fig. 5. The objective of the grinding program, for the first step, is to obtain in each grinding pass the same contact area S_{max} to maximize the MRR.

5.2 Calculation of the intersection surfaces

To place the first ellipse in the first layer (E1L1) (Fig. 5). The contact surface between the grinding wheel and the workpiece is calculated to insure a maximum material removal rate. This surface area is linked to the depth of cut d (9).

The robot is doing a back and forth motion along the y axis. Consequently, the contact area is function only of (x,z) position of the center of the grinding wheel.

The position of the next passes of the grinding wheel depends on the position of the previous passes. As a result of this, calculating the intersection between the ellipses of different layers is needed and can be done using work of [19].

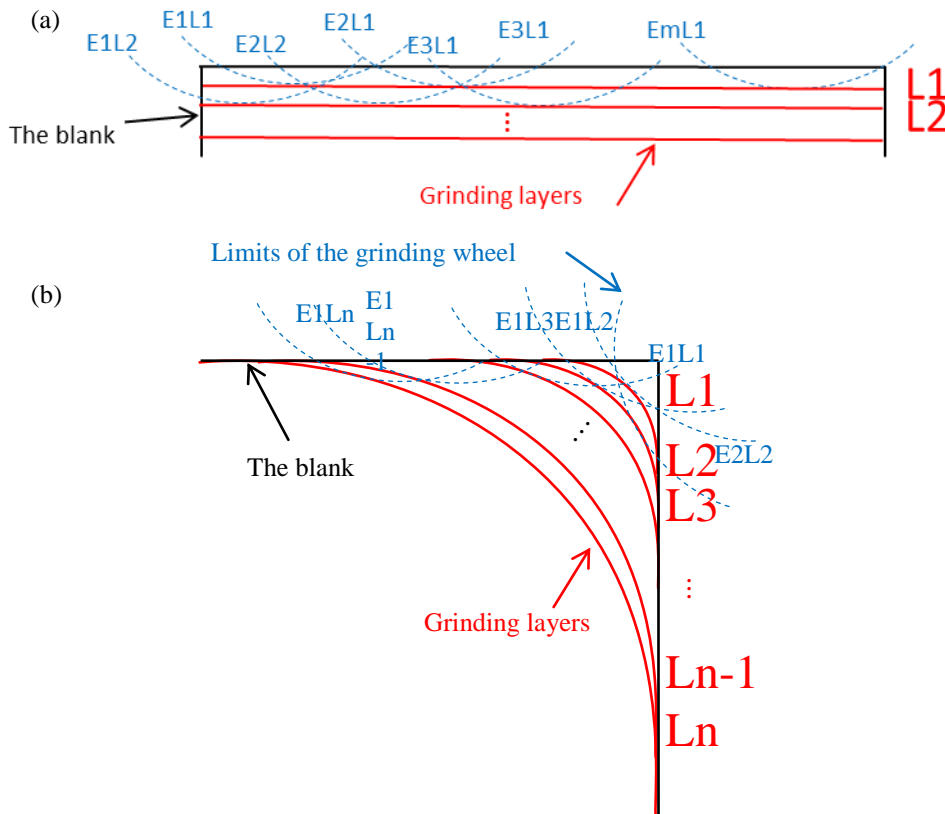


Fig. 5 The limits of the grinding wheel in different layers for (a) surfacing (b) corner grinding
 The number of layers N is dependent on the amount of material that has to ground (10). Where d_{max} is the maximum depth of cut.

$$N = \frac{R(\sqrt{2} - 1) + D}{d_{max}} \quad (10)$$

6 Grinding program

In order to determine the trajectory of the robot, it is necessary to determine the position of the grinding wheel as a function of time. Matlab program uses the grinding process parameters and the geometry of the ground workpiece to determine the robot path and to evaluate the quality of the final workpiece using the previously described method. This program needs as inputs: the grinding wheel dimensions, the grinding advance speed, the ground workpiece dimension and the grinding force parameter K (Fig. 6). The grinder rotation speed, material properties and other constant parameters are taken into consideration while determining the parameter K of the force model.

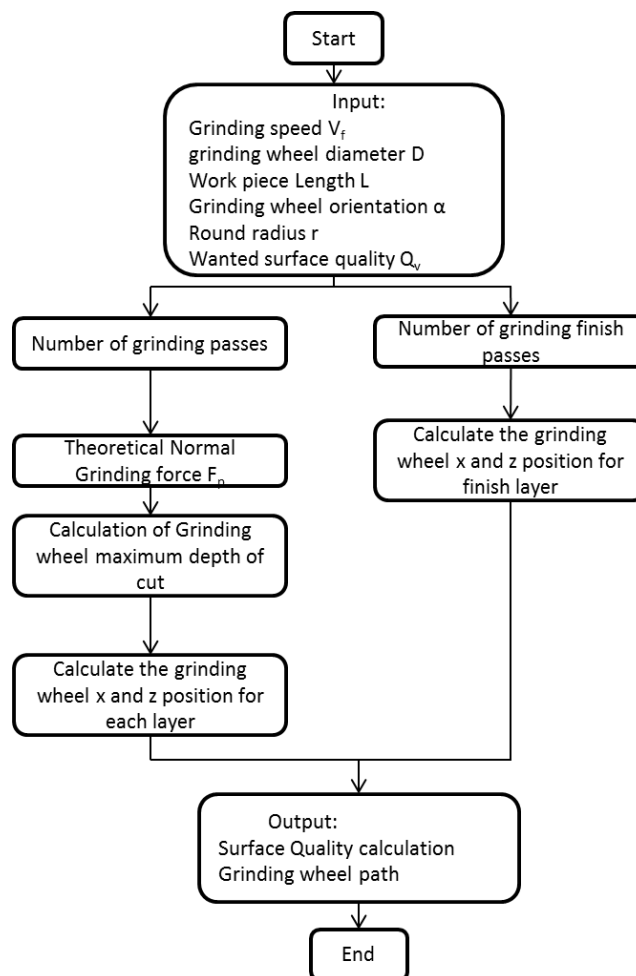


Fig. 6 Flow diagram of path planning and surface quality evaluation

7 Results

The number of passes and consequently the time needed for the grinding operation is directly linked to normal grinding force applied on the grinding wheel. Fig. 7 shows the effect of varying this parameter on the number of grinding pass and therefore on the efficiency of the process. Increasing the grinding force will

increase the area of the contact surface, therefore the number of passes and the time needed for the grinding operation decreases. Fig. 4 shows the tool path followed by the grinding wheel. The most important feature of the corner rounds along the width of the workpiece is the circularity C. The formula used to calculate this coefficient is (11).

$$C = \frac{p^2}{\pi \times A} \tag{11}$$

Where, P is the perimeter and A is the surface of rounds. The closer C is to 1, the closer the rounds surface is to a perfect quarter of a circle. In addition to that, the surface finish roughness is evaluated by Ra. Fixing the grinding force to 200N and the grinding feed speed to 0.5 m/s. we were able to achieve rounds circularity equal to 1.0021 and a medium radius of 4.005mm in simulation during the roughing step. For the finishing step, two different strategies are compared in order to choose the efficient one Fig. 8.

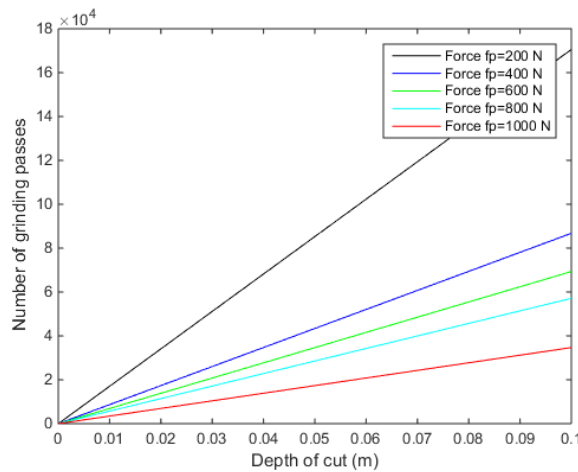


Fig. 7 Effect of grinding force on the efficiency of the process

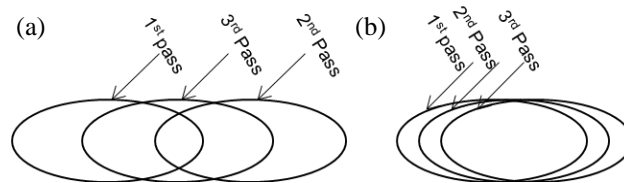


Fig. 8 Grinding wheel perimeter for 3 consecutive passes with (a) First finishing strategy (b) Second finishing strategy

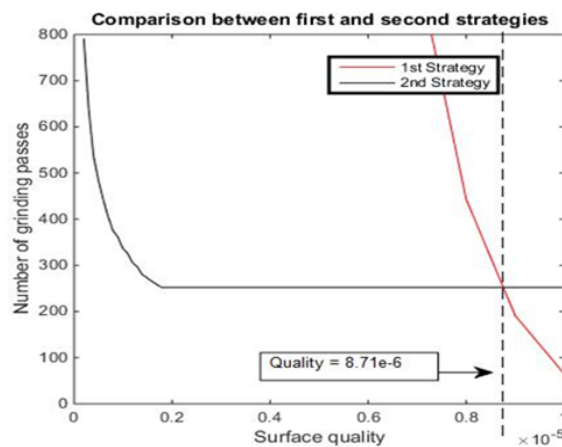


Fig. 9 Comparison between 1st and 2nd finish strategies

The most intuitive one is placing the second pass $j+1$ in the same radius as the previous one j but at a slightly bigger angle $\Delta\theta$ that is a function of the wanted surface quality: $\theta_{j+1} = \theta_j + \Delta\theta$. We can observe also, when done manually, that operators choose to place the $j+1$ pass between the two last pass j and $j-1$: $\theta_{j+1} = \frac{\theta_j + \theta_{j-1}}{2}$. The choice of the strategy depends on the wanted surface quality R_a (Fig. 9). The wanted surface quality we fixed is $R_a=5\mu\text{m}$, therefore the chosen grinding strategy for the finishing step is the 2nd. This step accounts for 40% of the time need in the robotic grinding operation. Fig. 10 shows a comparison between finished and unfinished rounds. The circularity is reduced from 1.0021 to 1.0001 and a medium radius of 4mm. using the path planning program we were able to estimate the corner grinding operation to be 10 min 56 s. Grinding the same workpiece manually will take approximately 20min to finish. The solution we propose helped reduce the time needed by 45%.

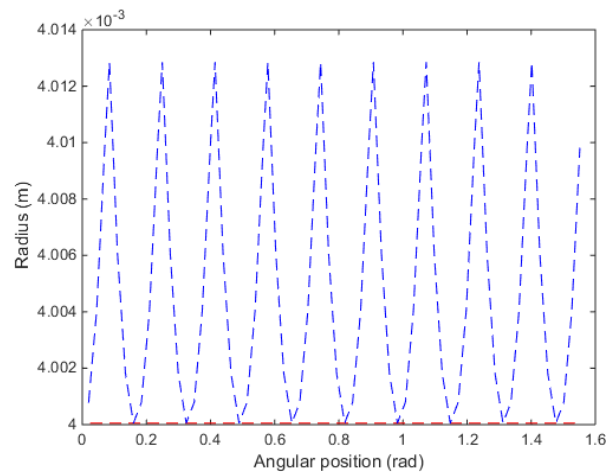


Fig. 10 Finished and unfinished workpiece in red and blue respectively

8 Conclusion

In this paper, we properly presented a robotic grinding solution that can be applied easily on different robots. This practical solution helped reduce vibrations and improve sufficiently surface quality. We proposed also a robotic path planning method that was implemented in a Matlab program. This program was used for surface and corner grinding of a parallelepiped workpiece. It was able to reliably produce the most efficient robot path for those operations. The grinding is done in two steps, to efficiently have a good finished surface. The next goal of this work is the experimental validation of the robotic grinding process and the actuator models, as well as the grinding method.

Acknowledgement

We would like to thank the Robotix Academy, contract number N°002-4-09-001 for funding this work as a part of the project funded by INTERREG V-A Grande Région program.

References

- [1] E.R. Andersson, Design and testing of a vibration attenuating handle, International journal of industrial ergonomics6 (1990) 119-125
- [2] H. Huang, Z.M. Gong, X.Q. Chen, L. Zhou, Robotic grinding and polishing for turbine-vane overhaul,

Journal of Materials Processing Technology 127 (2002) 140-145

- [3] M.C. Sozbilen, A.E. Dastan, H. Gunay, L. Kucuk, A prospective study of angle grinder injuries in the hands and forearms during a one-year period, *Hand Surgery and Rehabilitation* 37 (2018) 300-304
- [4] T. Thomessen, T.K. Lien, P.K. Sannæs, Robot control system for grinding of large hydro power turbines, *Industrial Robot: An International Journal* 28 (2001) 328-334
- [5] H. Dai, K.M. Yuen, M.A. Elbestawi, Parametric modelling and control of the robotic grinding process, *International Journal of Advanced Manufacturing Technology* 8 (1993) 182-192
- [6] M. Minami, T. Asakura, L.X. Dong, Y.M. Huang, Position control and explicit force control of constrained motions of a manipulator for accurate grinding tasks, *Advanced Robotics* 11 (1996) 285-300
- [7] H.K. Tönshoff, J. Peters, I. Inasaki, T. Paul, Modelling and Simulation of Grinding Processes, *CIRP Annals* 41 (1992) 677-688
- [8] U.S.P. Durgumahanti, V. Singh, P.V. Rao, A New Model for Grinding Force Prediction and Analysis, *International Journal of Machine Tools and Manufacture* 50 (2010) 231-240
- [9] E. Salje, Grundlagen des schleifvorganges, *Werkstatt und Betrieb* 86 (1953) 177-182
- [10] K. Brach, D.M. Pai, E. Ratterson, M.C. Shaw, Grinding forces and energy, *Journal of Engineering for Industry* 110 (1988) 25-31
- [11] K. Ono, Analysis of the grinding force, *Bulletin of the Japan Society of Grinding Engineers* 1 (1961) 19-22
- [12] R.P. Lindsay, On the metal removal and wheel removal parameters—surface finish, geometry and thermal damage in precision grinding, Thesis, Worcester Polytechnic Institute, 1971.
- [13] G. Werner, Influence of work material on grinding forces, *Annals of CIRP* 27 (1978) 243-248
- [14] H.-C. Chang, J.-J. A. Wang, A stochastic grinding force model considering random grit distribution, *International Journal of Machine Tools and Manufacture* 48 (2008) 1336-1344
- [15] W. Persoons, P. Vanherck, A Process Model for Robotic Cup Grinding, *CIRP Annals* 45 (1996) 319-325
- [16] H. Nasri, G. Bolmsjo, A process model for robotic disc grinding, *International Journal of Machine Tools and Manufacture* 35 (1995) 503-510
- [17] R.S. Hahn, R.P. Lindsay, The influence of process variables on material removal, surface integrity, surface finish and vibration in grinding, *Advances in Machine Tool Design and Research* (1969) 95-117
- [18] M.D. Chaoui, F. Léonard, G. Abba, Improving Surface Roughness in Robotic Grinding Process, *ROMANSY 22 – Robot Design, Dynamics and Control* 584 (2019) 363-369
- [19] P.J. Schneider, D.H. Eberly, Geometric tools for computer graphics, chapter 7. Morgan Kaufmann Publishers, United States of America, 2003